

Effect of transversely bedding layer on the biaxial failure mechanism of brittle materials

Hadi Haeri¹, Vahab Sarfarazi^{2a}, Zheming Zhu^{*1} and Ehsan Moosavi^{3b}

¹MOE Key Laboratory of Deep Underground Science and Engineering, School of Architecture and Environment, Sichuan University, Chengdu 610065, China

²Department of Mining Engineering, Hamedan University of Technology, Hamedan, Iran

³Department of Mining Engineering, Islamic Azad University, South Tehran Branch, Tehran, Iran

(Received April 7, 2018, Revised October 24, 2018, Accepted November 13, 2018)

Abstract. The biaxial failure mechanism of transversally bedding concrete layers was numerically simulated using a sophisticated two-dimensional discrete element method (DEM) implemented in the particle flow code (PFC2D). This numerical modelling code was first calibrated by uniaxial compression and Brazilian testing results to ensure the conformity of the simulated numerical model's response. Secondly, 21 rectangular models with dimension of 54 mm×108 mm were built. Each model contains two transversely bedding layers. The first bedding layer has low mechanical properties, less than mechanical properties of intact material, and second bedding layer has high mechanical properties, more than mechanical properties of intact material. The angle of first bedding layer, with weak mechanical properties, related to loading direction was 0°, 15°, 30°, 45°, 60°, 75° and 90° while the angle of second layer, with high mechanical properties, related to loading direction was 90°, 105°, 120°, 135°, 150°, 160° and 180°. Is to be note that the angle between bedding layer was 90° in all bedding configurations. Also, three different pairs of the thickness were chosen in models, i.e., 5 mm/10 mm, 10 mm/10 mm and 20 mm/10 mm. The result shows that in all configurations, shear cracks develop between the weaker bedding layers. Shear cracks angel related to normal load change from 0° to 90° with increment of 15°. Numbers of shear cracks are constant by increasing the bedding thickness. It's to be noted that in some configuration, tensile cracks develop through the intact area of material model. There is not any failure in direction of bedding plane interface with higher strength.

Keywords: transversely bedding layer; biaxial strength; PFC2D

1. Introduction

Anisotropy is one of the principal mechanical properties of various types of concretes. Weak planes may reduce the shear strength of concretes because they may cause large deformation due to anisotropic behavior of concretes (Park and Min, 2015). Therefore, the effect of discontinuities on the anisotropic behaviour of a jointed rock, such as the compressive and shear strength and, failure pattern, needs to be evaluated as part of safety assessments for any concrete engineering project.

Transverse anisotropy studies can be easily applied to engineering problems (Yu *et al.* 2013, Li 2013) when the concretes are bedded or layered. In terms of the mechanical properties of these types of concretes, anisotropic characteristics are usually studied by conducting some experimental works (Lei *et al.* 2013, Labiouse and Vietor 2014, Khanlari *et al.* 2014) and numerically simulated tests (Sun *et al.* 2011, Saeidi *et al.* 2013, Yu *et al.* 2013, Labiouse and Vietor 2014). The displacements (Sagong *et al.* 2011) and breaking procedures (Vietor *et al.* 2010, Seeska *et al.*

2011) are typically analyzed to discuss the anisotropic characteristics. Among such studies, Liang *et al.* (2005) investigated the mechanical properties and the failure process of stratified concretes using numerical code RFPA. They concluded that the orientation of layers may largely affect the breaking process of the concrete (i.e., the peak strength, fracturing modes and deformation characteristics of concretes are affected). Tavallali and Vervoort (2010) found that the layer orientation determined both the strength and failure modes of the concrete samples. Some experimental work has been conducted by Moradian *et al.* (2010) on the natural joints cored from an in situ rock mass to study the shear behaviour of concrete joints. The dominating influence of joints on the shear behaviour of a concrete mass was emphasized. Effects of anisotropy on the mechanical behavior of concretes were investigated by Dinh *et al.* (2013) and they numerically simulated the degree of anisotropy and concluded that it has a strong influence on the tensile strength of concrete or rock. The effects of inherently anisotropic concretes on their shear strengths were studied by Ghazvinian *et al.* (2013). According to their research, the anisotropic effect of the weak plane orientation is a significant occurrence that must be noted in analyse and failure mechanism studies. A large number of studies have been carried out to investigate the anisotropic behaviour of a cracked concrete under compressive, tension tests (Zhou *et al.* 2008, Zhou *et al.*

*Corresponding author, Professor
E-mail: zhemingzhu@hotmail.com

^aAssistant Professor

^bAssociate Professor

2014, Zhou *et al.* 2012, Zhou 2010, Kulatilake *et al.* 2001, Zhang *et al.* 2011a, b, Lancaster *et al.* 2013, Mobasher *et al.* 2014, Haeri *et al.* 2014, Lisjak *et al.* 2014a, Noel and Soudki 2014, Oliveira and Leonel 2014, Kim and Taha 2014, Tiang *et al.* 2015, Wan Ibrahim *et al.* 2015, Liu *et al.* 2015, Potyondy 2015, Haeri 2015, Haeri *et al.* 2015a, b, c, Yang *et al.* 2015, Silva *et al.* 2015, Gerges *et al.* 2015, Fan *et al.* 2016, Li *et al.* 2016, Sardemir 2016, Sarfarazi *et al.* 2016, Haeri *et al.* 2016a, b, c, Haeri and Sarfarazi 2016, Shuraim 2016, Shaowei *et al.* 2016, Wang *et al.* 2016, 2017, Zhou and Bi 2018), whereas studies of anisotropic shear behaviour remain limited. Many researchers have studied the shear behaviours of concrete samples with pre-existing cracks (Yun *et al.* 2013, Wasantha *et al.* 2014, Sardemir 2016, Sarfarazi *et al.* 2016, Shuraim 2016, Wang *et al.* 2016). However, the anisotropy of the shear behaviour of a jointed concrete mass with discrete fractures is controlled by the complex interactions of joints and intact-rock bridges. In addition, the geometry of discontinuities can exert a controlling influence on the distribution of fractured zones (Li 2013, Labiouse and Vietor 2014). Theories or modelling methods related to the evaluation of a natural rock mass with randomly distributed discontinuities are still limited. Yang *et al.* (2015) proposed an efficient technique to evaluate the mechanical characteristics of concrete. The constitutive relationship and failure mechanisms were introduced, and the proposed model was verified using a case study. This approach is suitable for the stability analysis of concrete engineering based on numerical simulations. The key of their research is to evaluate the scale effects (Min and Jing 2003), anisotropy and directionality of the representative elementary volume (REV) of a fractured concrete. The mechanical properties in their model were investigated by numerically conducting a uniaxial compressive test using the RFPA code. Shear behaviour is also one of the most important properties of a jointed rock mass. Thus, the anisotropy and scale effect of shear behaviours should also be discussed. Some efficient numerical methods have been developed to study the concrete failure process, such as RFPA (Tang 1997, Tang *et al.* 2000), to study the crack propagation and fracture patterns of concrete materials under stress, such as the particle flow code (PFC) by Cundall and Strack (1979), and to analyse the crack growth of complex crack patterns, such as the cracking-particle method (Rabczuk and Belytschko 2004, Rabczuk and Belytschko 2007, Rabczuk *et al.* 2010), dual-horizon peridynamics (Ren *et al.* 2016) and dual-support smoothed particle method (Dai *et al.* 2016). These numerical methods have many advantages in the modelling of rock masses that possess the ability to fracture and break apart under stress. For the purpose of a quantitative description, numerical analyses are carried out using PFC2D version 3.0, which has been shown to have advantages in the simulation of mechanical behaviours of concretes (Lambert *et al.* 2010, Zhang *et al.* 2011a, b) and discontinuities in fractured rock masses (Potyondy and Cundall 2004, Park and Min 2015, Potyondy 2015, Wang *et al.* 2016). PFC2D models the movement and interaction of circular particles by the discrete element method. In this approach, each concrete sample is represented as an

assemblage of circular disks which are confined by planar walls. Then the interface forces and particles motions within this assembly are modeled. In this modelling technique each particle can move independently and may interact at its contacts with the others. Generally, two basic bonding models are adopted in PFC2D i.e., a contact-bonding model and a parallel-bonding model (Itasca Consulting Group, Inc. 2004). These models may be considered as a kind of glue joining the particles to each other. The moments transmission in between the particles can be effectively modeled by the parallel bonding model therefore the constitutive equations for the cementitious materials such as rocks and concretes can be well described. However, the model calibration may need some more parameters. On the other hand, in the contact bonding model, the contact bonds might be envisaged as elastic springs with constant normal and shear stiffness acting at each contact point. The feasibility of the contact bonding model is verified by Hazzard and Young (2000).

These two models may be used to reproduce the mechanical behaviors on different concrete types, therefore, it may be logical to use PFC2D as a modelling device to investigate the effects of anisotropy on the shearing behaviors of concretes and rocks.

Objective of this paper is to evaluate the effect of transversely bedding layers angle and its thickness on the strength and failure behavior of transversely isotropic concretes. This performed by particle flow code in two dimension, PFC2D.

2. Numerical simulation

2.1 Bonded particle model and Particle Flow Code 2D (PFC2D)

Particle flow code in two dimensions (PFC2D) is a distinct element code that represents the material as an assembly of rigid particles which can move independently of one another and interact only at contacts (Itasca 1999 version 3.1, Potyondy and Cundall 2004). The movements and interaction forces of particles are calculated by use of a central finite difference method as applied in the DEM. For models of the contacts, both linear and non-linear contact models with frictional sliding can be used. The linear contact model, which was used in this study, provides an elastic relationship between the relative displacements and contact forces of particles. The basic contact model in the PFC code (contact force-displacement relationship) is the linear point contact between two particles, relating contact normal force component, F^n , contact overlap, U^n , increment of shear force, ΔF^s , and shear displacements, ΔU^s , and given by

$$\begin{cases} F^n = K^n U^n \\ \Delta F^s = -k^s \Delta U^s \end{cases} \quad (1)$$

where K^n and k^s are the contact normal and shear stiffness, respectively. The frictional strength of the contact is given by

$$F^s \leq \mu F^n \quad (2)$$

where μ is the friction coefficient between particles. Point contact models represented by Eq. (1) can only consider relative motion between individual particles. However, when a group of bounded particles must be considered as a whole, cemented contact including both contact forces and torques are needed. In such a case, the relationships between the above incremental quantities become

$$\begin{cases} \Delta \bar{F}^n = \bar{k}^n A \Delta U^n \\ \Delta \bar{F}^s = -\bar{k}^s A \Delta U^s \end{cases} \quad (3)$$

And

$$\begin{cases} \Delta \bar{M}^n = -\bar{k}^s J \Delta \theta^n \\ \Delta \bar{M}^s = -\bar{k}^n I \Delta \theta^s \end{cases} \quad (4)$$

where F^n , F^s , M^n and M^s are the force components and torques (moments) about the center of the cemented-contact zone, k^n and k^s are normal and shear bond stiffness per unit area, θ^n and θ^s are the components of rotation angle, and A , I , and J are the area, moment of inertia, and polar moment of inertia of the bond cross-section, respectively. The strength of the cemented contact is then written as

$$\begin{aligned} \bar{\sigma}^{\max} &= \frac{-\bar{F}^n}{A} + \frac{|\bar{M}^s| \bar{R}}{I} < \bar{\sigma}_c \\ \bar{\tau}^{\max} &= \frac{-\bar{F}^s}{A} + \frac{|\bar{M}^n| \bar{R}}{J} < \bar{\tau}_c \end{aligned} \quad (5)$$

where R is the radius of the cemented zone, σ_c and τ_c are the tensile and shear strength of the cemented contact, respectively. Young's modulus for particle contacts E_c and particle bondage \bar{E}_c are defined to relate the contact and bond stiffness as follows

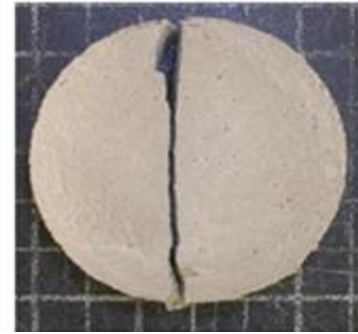
$$\begin{aligned} E_c &= \frac{k_n}{2t} \quad (t = 1 \text{ in } 2D) \\ \bar{E}_c &= \bar{k}_n (R^{(A)} + R^{(B)}) \end{aligned} \quad (6)$$

where $R^{(A)}$ and $R^{(B)}$ are radii of circular particles in contact. In the PFC code, cemented contacts as expressed in Eqs. (3)-(8) are called parallel bonds. By using the parallel bond model it is possible to reproduce the mechanical properties of a rock-like material.

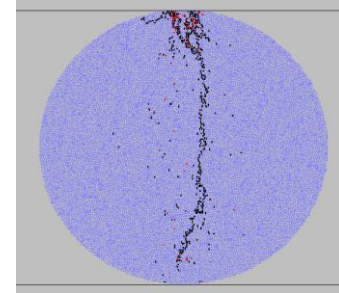
To generate a parallel-bonded particle model for PFC2D, using the routines provided (Itasca 1999, version 3.1), the following micro properties should be defined: ball-to-ball contact modulus, stiffness ratio k_n over k_s , ball friction coefficient, parallel normal bond strength, parallel shear bond strength, ratio of standard deviation to mean of bond strength both in normal and shear direction, minimum Ball radius, parallel-bond radius multiplier, parallel-bond modulus, and parallel-bond stiffness ratio. To establish the appropriate micro properties to be used for the particle assembly, it is necessary to conduct a calibration procedure. The particle contact properties and bonding characteristics cannot be determined directly from tests performed on laboratory model samples. The material properties

Table 1 Micro properties used to represent the intact concrete

Parameter	Value	Parameter	Value
Type of particle	disc	Parallel bond radius multiplier	1
density	3000	Young modulus of parallel bond (GPa)	40
Minimum radius	0.27	Parallel bond stiffness ratio	1.7
Size ratio	1.56	Particle friction coefficient	0.4
Porosity ratio	0.08	Parallel bond normal strength, mean (MPa)	70
Damping coefficient	0.7	Parallel bond normal strength, SD (MPa)	2
Contact young modulus (GPa)	40	Parallel bond shear strength, mean (MPa)	70
Stiffness ratio	1.7	Parallel bond shear strength, SD (MPa)	2



(a)



(b)

Fig. 1 Failure pattern in (a) physical sample, (b) PFC2D model

Table 2 Brazilian tensile strength of physical and numerical samples

Physical tensile strength (MPa)	4.5 and 4.7
Numerical tensile strength (MPa)	4.5

Table 3 micro properties of low and high strength of bedding layer interfaces

Parameter	Low Value	High value	Parameter	Low value	High value
n_bond (MPa)	1e3	1e8	s_bond (MPa)	1e3	1e8
fric	0.25	0.5			

determined by laboratory experimentation are macro-mechanical in nature because they reflect continuum

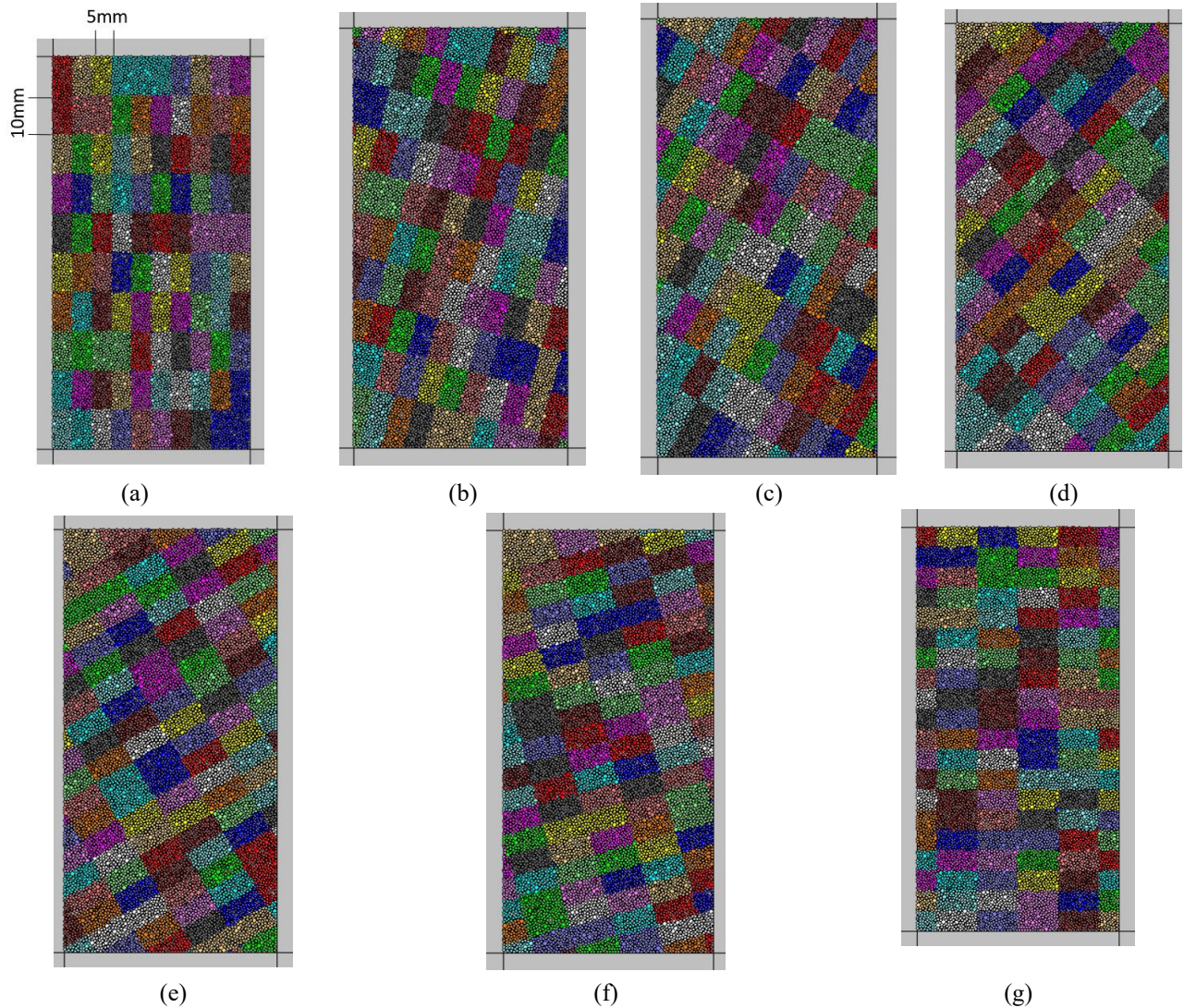


Fig. 3 anisotropic concrete with layers thicknesses of 5 mm and layer angle of (a) 0° , (b) 15° , (c) 30° , (d) 45° , (e) 60° , (f) 75° and (g) 90°

behavior. An inverse modeling procedure was used to determine the appropriate micro-mechanical properties of the numerical models from the macro-mechanical properties determined in the laboratory tests. The trial-and-error approach is one of the methods used to relate these two sets of material property (Itasca 1999). It involves assumption of micro-mechanical property values and comparison of the strength and deformation characteristics of the numerical models with those of the laboratory samples. The micro-mechanical property values that give a simulated macroscopic response close to that of the laboratory tests are then adopted for the discontinuous jointed blocks.

2.2 Preparing and calibrating the numerical model

The uniaxial compression and Brazilian tensile tests were used to calibrate the tensile strength of the specimens modelled in the PFC2D. The particle assembly is modelled in a general discrete element method like PFC2D by considering these four important steps: (a) generation and packing of the particles, (b) installation of an isotropic stress field, (c) elimination of floating particles, and (d)

installation of the particles bonds. An inverse modeling technique based on the trial and error approach is adopted in PFC2D (Itasca 1999) to determine the appropriate micro mechanical properties of the particle assembly from the macro mechanical properties given by the experimental tests for the numerical simulation of any geo-mechanical problem.

The particle assembly in a PFC bonding model can be appropriately calibrated by adopting the micro-properties listed in Table 1 and using the standard calibration procedures proposed by Potyondy and Cundall (2003). The diameter of the numerically simulated Brazilian disc was 54 mm and about 5,615 particles were considered in a single disc specimen. Then, the lateral walls of the specimen were moved toward each other with a speed of 0.016 m/s so that the disc was crushed. The failure process and fracturing patterns of the numerically and experimentally tested samples are given in Figs. 1(a) and 1(b), respectively. These figures illustrate that the failure planes obtained from the numerically modelled samples and the corresponding laboratory testing specimens are well matching with each

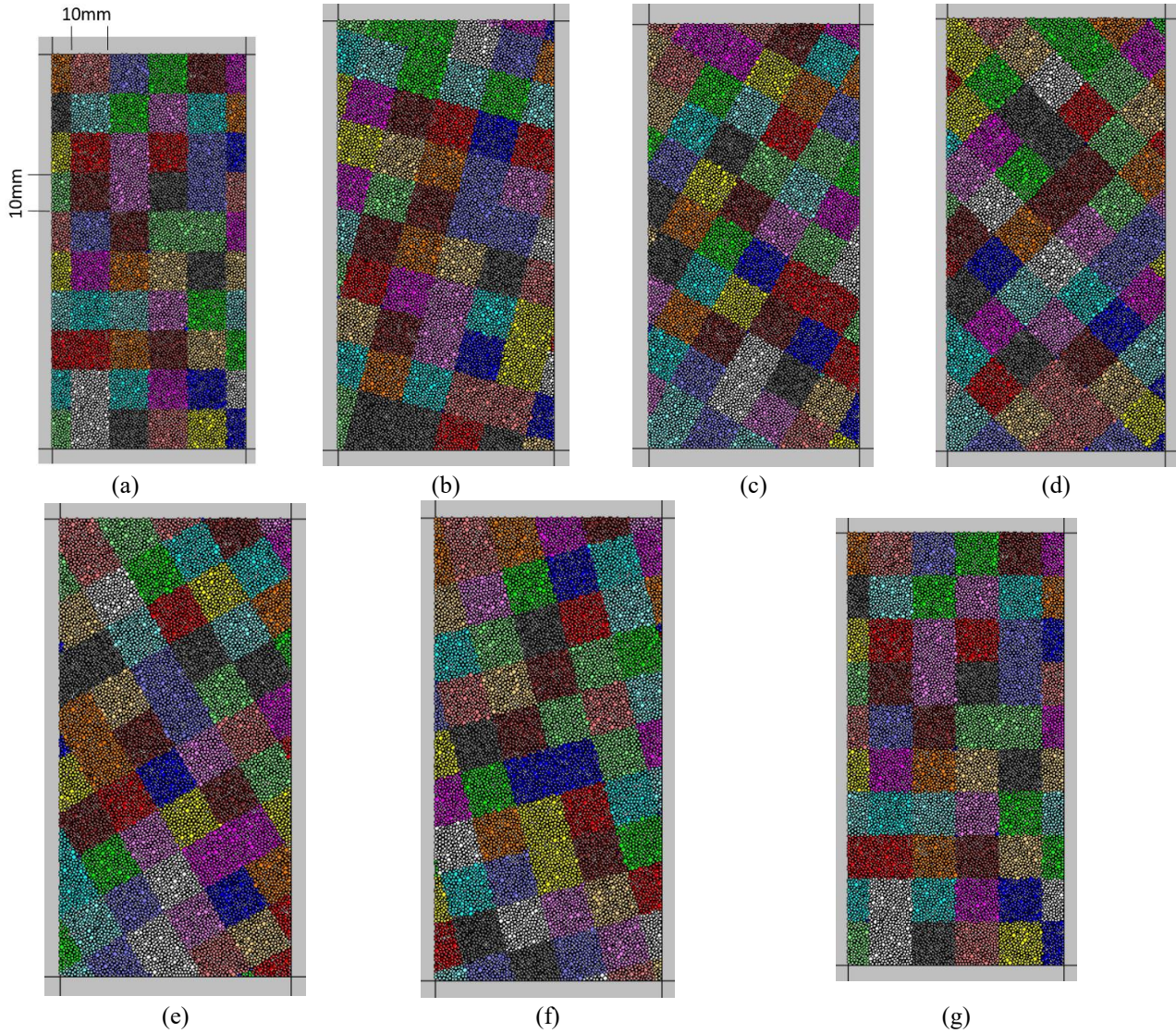


Fig. 4 Anisotropic concrete with Layers thicknesses of 10 mm and layer angle of (a) 0° , (b) 15° , (c) 30° , (d) 45° , (e) 60° , (f) 75° and (g) 90°

other. The numerically estimated tensile strengths of the modelled samples are compared with those gained from the corresponding experimental measurements and presented in Table 2 with a good agreement between the numerical and experimental results.

2.3 model preparation using Particle Flow Code

After calibration of PFC2D, tensile tests on transverse bedding layers were numerically simulated by creating a hollow disc model in PFC2D (by using the calibrated micro parameters) (Figs. 3, 4 and 5). The internal and external radius of hollow disc was 15 mm and 5 mm, respectively. A total of 11179 disks with a minimum radius of 0.27 mm were used to make up the specimen. The particles are surrounded by two loading walls. Transversely bedding layers consisted of two unparallel bedding layers. The angle of first bedding layer, with weak mechanical properties, related to loading direction was 0° (Fig. 3(a)), 15° (Fig. 3(b)), 30° (Fig. 3(c)), 45° (Fig. 3(d)), 60° (Fig. 3(e)), 75° (Fig. 3(f)) and 90° (Fig. 3(g)) while the angle of

second layer, with high mechanical properties, related to loading direction was 180° . It is to be noted that the angle between bedding layer was 90° in all bedding configurations. Also, three different pairs of the thickness were chosen in models, i.e., 5 mm/10 mm (Fig. 3(a)), 10 mm/10 mm (Fig. 4(a)), and 20 mm/10 mm (Fig. 5(a)). The models are under confining pressure of 1 MPa. The disk was crushed by lateral walls, moving towards each other with a low speed of 0.016 m/s. Micro-properties of two different bedding layer interfaces were chosen too low and too high (Table 3).

3. Results

3.1 The effect of bedding layers angle on the failure mechanism of models

Figs. 6, 7 and 8 show the effect of transversely bedding layer on the failure pattern of models for bedding thickness of 5 mm/10 mm, 10 mm/10 mm and 20 mm/10 mm,

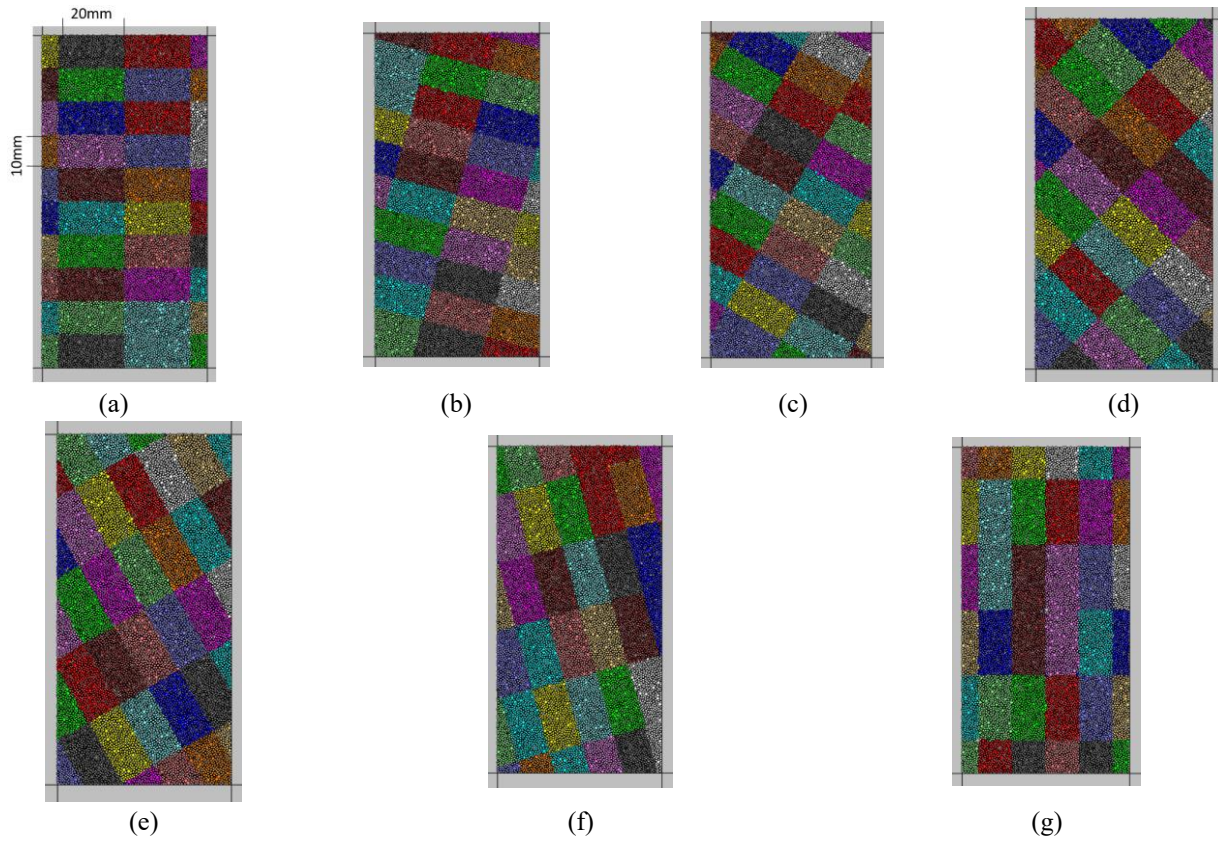


Fig. 5 Anisotropic concrete with Layers thicknesses of 5 mm and layer angle of (a) 0° , (b) 15° , (c) 30° , (d) 45° , (e) 60° , (f) 75° and (g) 90°

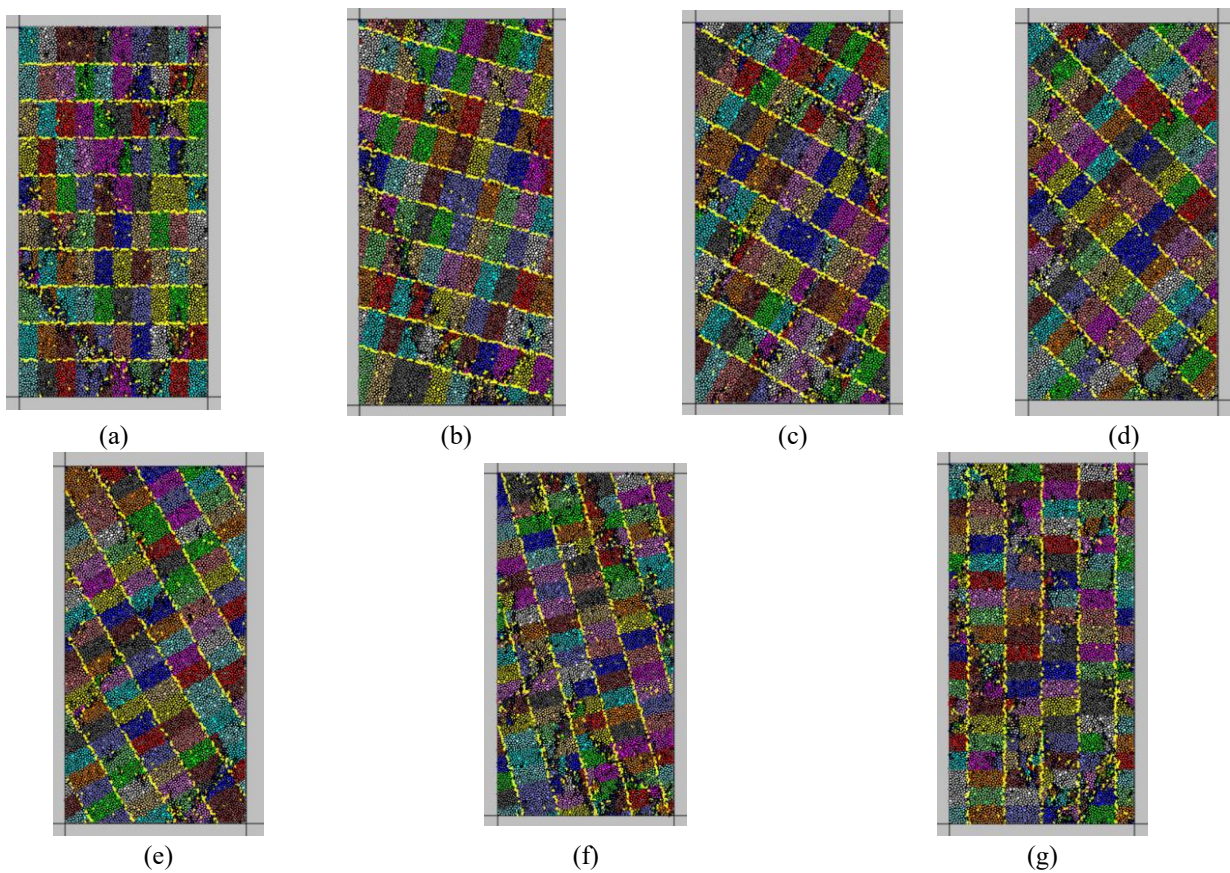


Fig. 6 Failure pattern in anisotropic concrete with layers thicknesses of 5 mm and layer angle of (a) 0° , (b) 15° , (c) 30° , (d) 45° , (e) 60° , (f) 75° and (g) 90°

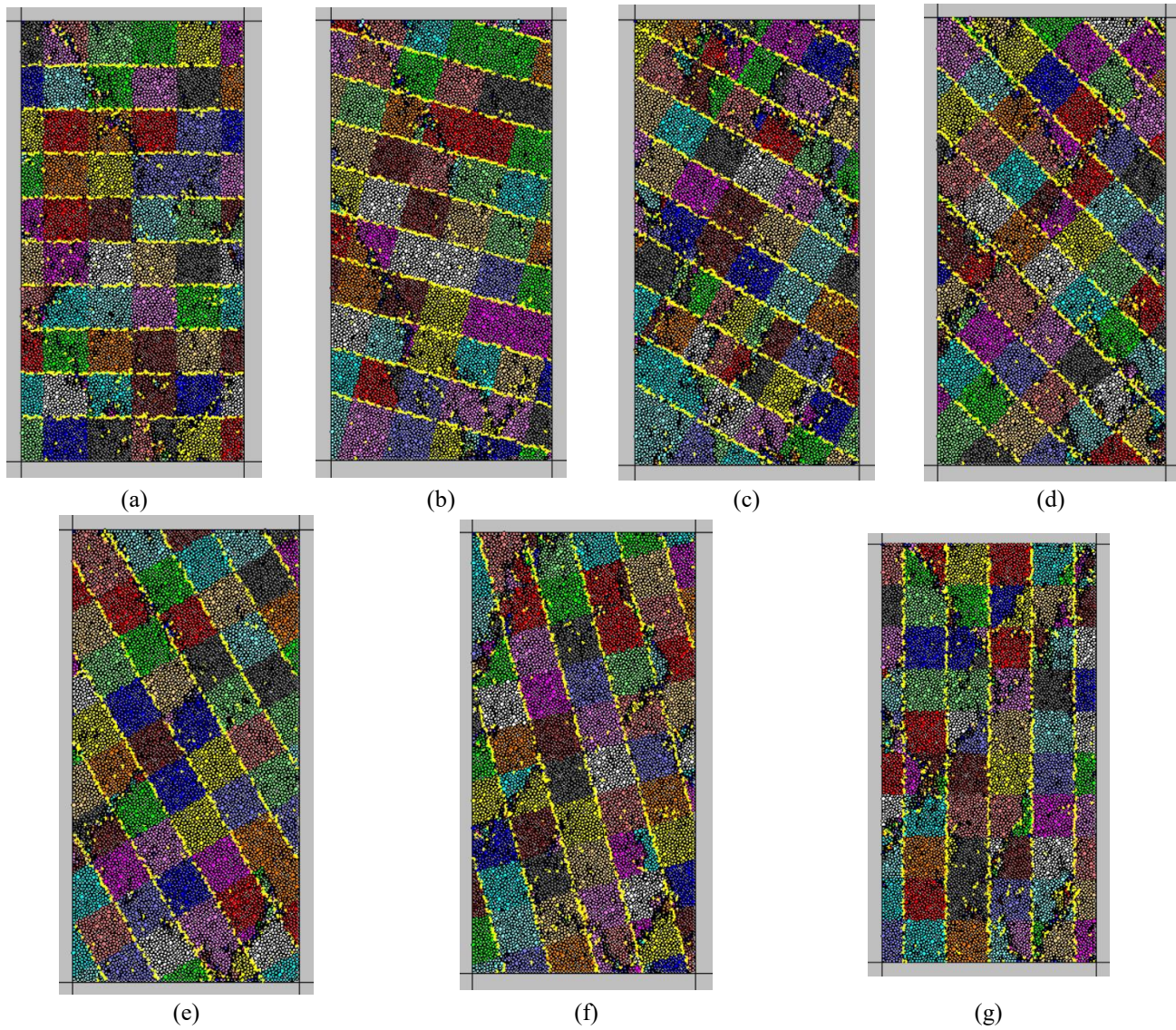


Fig. 7 Failure pattern in anisotropic concrete with layers thicknesses of 10 mm and layer angle of (a) 0° , (b) 15° , (c) 30° , (d) 45° , (e) 60° , (f) 75° and (g) 90°

respectively. In each figure the results of interfaces angularities have been shown. Yellow line and black line represent the shear crack and tensile crack, respectively. In all configurations, shear cracks develop between the weaker bedding layers. Shear cracks angle related to normal load change from 0° to 90° with increment of 15° . Numbers of shear cracks are constant by increasing the bedding thickness. It's to be noted that in some configuration, tensile cracks develop through the intact area of material model. There is not any failure in direction of bedding plane interface with higher strength.

4.2 The effect of bedding layer on the biaxial compressive strength

Fig. 9 shows the effect of transversely bedding layer on the biaxial compression strength for bedding thickness of 5 mm/10 mm, 10 mm/10 mm and 20 mm/10 mm, respectively. In this figure the results of interfaces

angularities have been shown. The minimum biaxial compression strength was occurred when weaker interface angle is between the 30° and 60° . The maximum value occurred in 90° . Also, the biaxial compression strength was increased by increasing the layer thickness.

4. Conclusions

In this work, the failure mechanisms of transversally bedding layers were numerically simulated by using PFC2D. Firstly, numerical model was calibrated by uniaxial, Brazilian experimental results to ensure the conformity of the simulated numerical model's response. Secondly, 21 circular models with dimension of 54 mm \times 108 mm were built. Each model contains two transversely bedding layers. The first bedding layer has low mechanical properties, less than mechanical properties of intact material, and second bedding layer have high

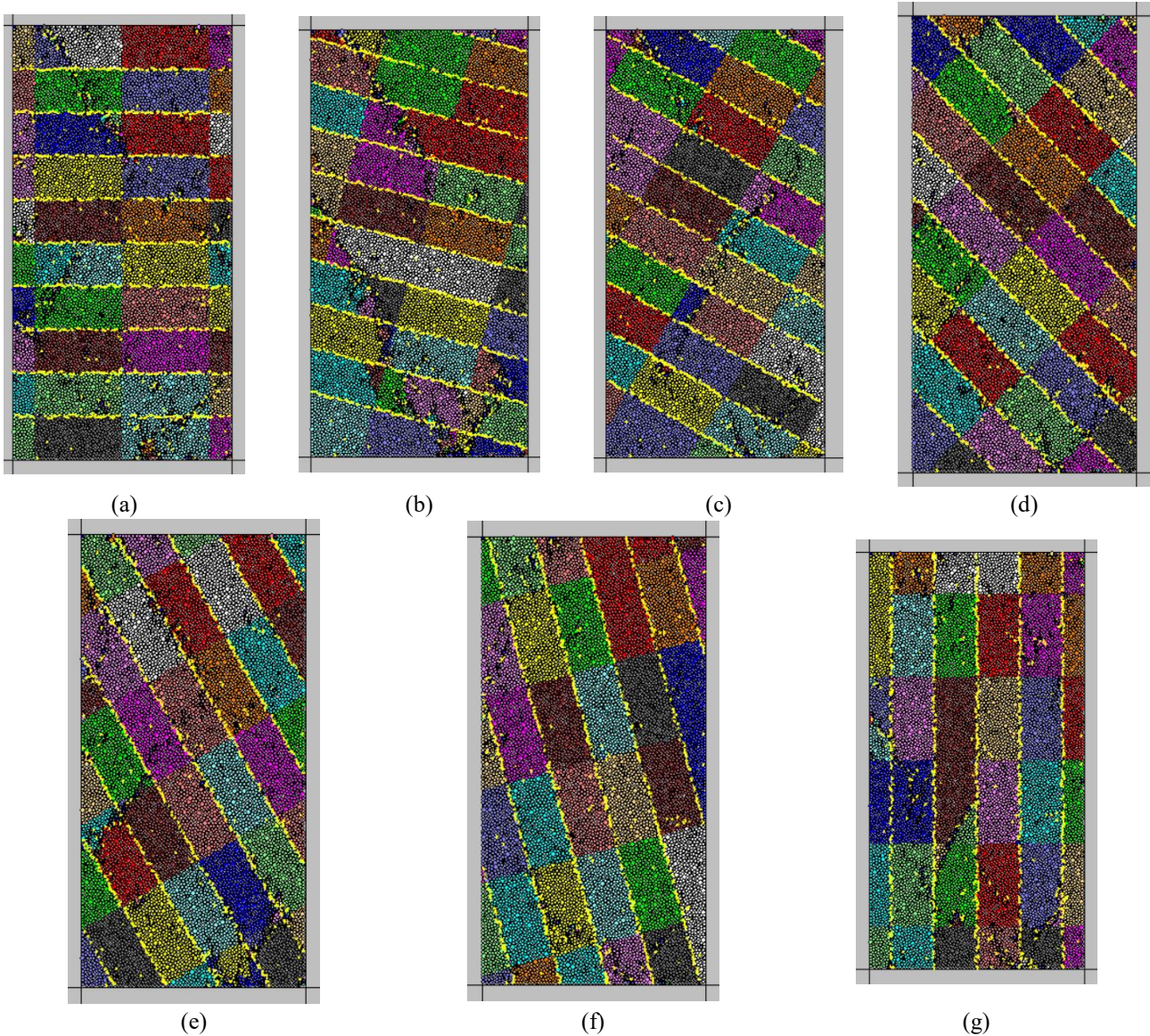


Fig. 8 Failure pattern in anisotropic concrete with layers thicknesses of 20 mm and layer angle of (a) 0°, (b) 15°, (c) 30°, (d) 45°, (e) 60°, (f) 75° and (g) 90°

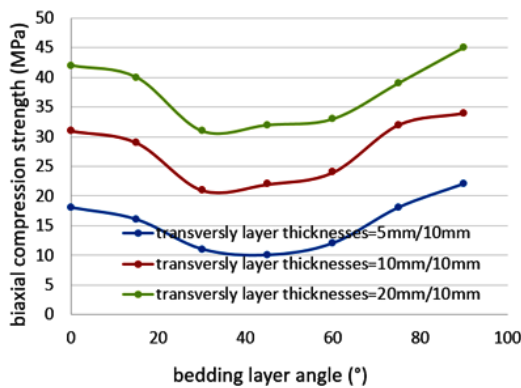


Fig. 9 the effect of bedding layer on the biaxial compression strength

mechanical properties, more than mechanical properties of intact material. The angle of first bedding layer, with weak mechanical properties, related to loading direction was 0°,

15°, 30°, 45°, 60°, 75° and 90° while the angle of second layer, with high mechanical properties, related to loading direction was 90°, 105°, 120°, 135°, 150°, 160° and 180°. It is to be noted that the angle between bedding layer was 90° in all bedding configurations. Also, three different pairs of the thickness were chosen in models, i.e., 5 mm/10 mm, 10 mm/10 mm and 20 mm/10 mm. The result shows that:

- In all configurations, shear cracks develop between the weaker bedding layers.
- Shear cracks angel related to normal load change from 0° to 90° with increment of 15°.
- Numbers of shear cracks are constant by increasing the bedding thickness.
- It's to be noted that in some configuration, tensile cracks develop through the intact area of material model.
- There is not any failure in direction of bedding plane interface with higher strength.
- The minimum biaxial strength was occurred when

weaker interface angle is between the 30° and 60°. The maximum value occurred in 90°.

- Also, the biaxial strength was increased by increasing the layer thickness.

References

- Cundall, P.A. and Strack, O.D. (1979), "A discrete numerical model for granular assemblies", *Geotech.*, **29**(1), 47-65.
- Dai, Z., Ren, H., Zhuang, X. and Rabczuk, T. (2016), "Dual-support smoothed particle hydrodynamics for elastic mechanics", *Int. J. Comput. Meth.*, **14**(4), 1750039.
- Dinh, Q.D., Heinz, K. and Martin, H. (2013), "Brazilian tensile strength tests on some anisotropic rocks", *Int. J. Rock Mech. Min. Sci.*, **58**, 1-7.
- Ghazvinian, A., Vaneghi, R.G., Hadei, M.R. and Azinfar, M.J. (2013), "Shear behavior of inherently anisotropic rocks", *Int. J. Rock Mech. Min. Sci.*, **61**, 96-110.
- Haeri, H. (2015), "Propagation mechanism of neighboring cracks in rock-like cylindrical specimens under uniaxial compression", *J. Min. Sci.*, **51**(3), 487-496.
- Haeri, H. (2016), "Propagation mechanism of neighboring cracks in rock-like cylindrical specimens under uniaxial compression", *J. Min. Sci.*, **51**(5), 1062-1106.
- Haeri, H. and Sarfarazi, V. (2016), "The effect of non-persistent joints on sliding direction of rock slopes", *Comput. Concrete*, **17**(6), 723-737.
- Haeri, H., Khaloo, A. and Marji, M.F. (2015a), "Experimental and numerical simulation of the microcrack coalescence mechanism in rock-like materials", *Strength Mater.*, **47**(5), 740-754.
- Haeri, H., Khaloo, A. and Marji, M.F. (2015b), "Fracture analyses of different pre-holed concrete specimens under compression", *Acta Mech. Sinic.*, **31**(6), 855-870.
- Haeri, H., Khaloo, A. and Marji, M.F. (2015c), "A coupled experimental and numerical simulation of rock slope joints behavior", *Arab. J. Geosci.*, **8**(9), 7297-7308.
- Haeri, H., Sarfarazi, V. and Hedayat, A. (2016a), "Suggesting a new testing device for determination of tensile strength of concrete", *Struct. Eng. Mech.*, **60**(6), 939-952.
- Haeri, H., Sarfarazi, V. and Lazemi, H. (2016b), "Experimental study of shear behavior of planar non-persistent joint", *Comput. Concrete*, **17**(5), 639-653.
- Haeri, H., Sarfarazi, V., Fatehi, M., Hedayat, A. and Zhu, Z. (2016c), "Experimental and numerical study of shear fracture in brittle materials with interference of initial double", *Acta Mech. Soil. Sinic.*, **29**(5), 555-566.
- Haeri, H., Shahriar, K. and Marji, M.F. (2013), "Modeling the propagation mechanism of two random micro cracks in rock samples under uniform tensile loading", *Proceedings of the ICF13*.
- Haeri, H., Shahriar, K., Fatehi Marji, M. and Moarefvand, P. (2014), "On the crack propagation analysis of rock like Brazilian disc specimens containing cracks under compressive line loading", *Lat. Am. J. Sol. Struct.*, **11**(8), 1400-1416.
- Hazzard, J.F. and Young, R.P. (2000), "Simulation acoustic emissions in bonded-particle models of rock", *Int. J. Rock Mech. Min. Sci.*, **37**, 867-872.
- Itasca Consulting Group, Inc. (2004), *Particle Flow Code in 2-Dimensions: Problem Solving with PFC2D*, Version 3.1, Itasca Consulting Group, Inc., Minneapolis.
- Jiang, Q., Feng, X.T., Hatzor, Y.H., Hao, X.J. and Li, S.J. (2014), "Mechanical anisotropy of columnar jointed basalts: An example from the Baihetan hydropower station", *Chin. Eng. Geol.*, **175**, 35-45.
- Khanlari, G.R., Heidari, M., Sepahigero, A.A. and Fereidooni, D. (2014), "Quantification of strength anisotropy of metamorphic rocks of the Hamedan province, Iran, as determined from cylindrical punch, point load and Brazilian tests", *Eng. Geol.*, **169**, 80-90.
- Kulatilake, P.H.S.W., Malama, B. and Wang, J.L. (2001), "Physical and particle flow modeling of jointed rock block behavior under uniaxial loading", *Int. J. Rock Mech. Min. Sci.*, **38**(5), 641-657.
- Labiose, V. and Vietor, T. (2014), "Laboratory and in situ simulation tests of the excavation damaged zone around galleries in Opalinus clay", *Rock Mech. Rock Eng.*, **47**(1), 57-70.
- Lambert, C., Buzzi, O. and Giacomini, A. (2010), "Influence of calcium leaching on the mechanical behavior of a concrete-mortar interface: A DEM analysis", *Comput. Geotech.*, **37**(3), 258-266.
- Lancaster, I.M., Khalid, H.A. and Kougioumtzoglou, I.A. (2013), "Extended FEM modelling of crack propagation using the semi-circular bending test", *Constr. Build. Mater.*, **48**, 270-277.
- Lei, M.F., Peng, L.M., Shi, C.H. and Wang, S.Y. (2013), "Experimental study on the damage mechanism of tunnel structure suffering from sulfate attack", *Tunn. Undergr. Space Technol.*, **36**, 5-13.
- Li, S., Wang, H., Li, Y., Li, Q., Zhang, B. and Zhu, H. (2016), "A new mini-grating absolute displacement measuring system for static and dynamic geomechanical model tests", *Measure.*, **82**, 421-431.
- Liang, Z.Z., Tang, C.A., Li, H.X., Xu, T. and Yang, T.H. (2005), "A numerical study on failure process of transversely isotropic rock subjected to uniaxial compression", *Rock Soil Mech.*, **26**(1), 57-62.
- Lisjak, A., Grasselli, G. and Vietor, T. (2014a), "Continuum-discontinuum analysis of failure mechanisms around unsupported circular excavations in anisotropic clay shales", *Int. J. Rock Mech. Min. Sci.*, **65**, 96-115.
- Liu, X., Nie, Z., Wu, S. and Wang, C. (2015), "Self-monitoring application of conductive asphalt concrete under indirect tensile deformation", *Case Stud. Constr. Mater.*, **3**, 70-77.
- Min, K.B. and Jing, L. (2003), "Numerical determination of the equivalent elastic compliance tensor for fractured rock masses using the distinct element method", *Int. J. Rock Mech. Min. Sci.*, **40**(6), 795-816.
- Moradian, Z.A., Ballivy, G., Rivard, P., Grave, L.C. and Rousseau, B. (2010), "Evaluating damage during shear tests of rock joints using acoustic emission", *Int. J. Rock Mech. Min. Sci.*, **47**(4), 590-598.
- Park, B. and Min, K.B. (2015), "Bonded-particle discrete element modeling of mechanical behavior of transversely isotropic rock", *Int. J. Rock Mech. Min. Sci.*, **76**, 243-255.
- Potyondy, D.O. (2015), "The bonded-particle model as a tool for rock mechanics research and application: Current trends and future directions", *Geosyst. Eng.*, **18**(1), 1-28.
- Potyondy, D.O. and Cundall, P.A. (2004), "A bonded-particle model for rock", *Int. J. Rock Mech. Min. Sci.*, **41**(8), 1329-1364.
- Rabczuk, T. and Belytschko, T. (2004), "Cracking particles: A simplified meshfree method for arbitrary evolving cracks", *Int. J. Numer. Meth. Eng.*, **61**(13), 2316-2343.
- Rabczuk, T. and Belytschko, T. (2007), "A three-dimensional large deformation meshfree method for arbitrary evolving cracks", *Comput. Meth. Appl. Mech. Eng.*, **196**(29-30), 2777-2799.
- Rabczuk, T., Zi, G., Bordas, S. and Hung, N.X. (2010), "A simple and robust three-dimensional cracking-particle method without enrichment", *Comput. Meth. Appl. Mech. Eng.*, **199**(37-40), 2437-2455.
- Ren, H., Zhuang, X., Cai, Y. and Rabczuk, T. (2016), "Dual-horizon peridynamics", *Int. J. Numer. Meth. Eng.*, **108**(12), 1451-1476.

- Saeidi, O., Stille, H. and Torabi, R.S. (2013), "Numerical and analytical analyses of the effects of different joint and grout properties on the rock mass groutability", *Tunn. Undergr. Space Technol.*, **38**, 11-25.
- Sagong, M., Park, D., Yoo, J. and Lee, J.S. (2011), "Experimental and numerical analyses of an opening in a jointed rock mass under biaxial compression", *Int. J. Rock Mech. Min. Sci.*, **48**(7), 1055-1067.
- Sardemir, M. (2016), "Empirical modeling of flexural and splitting tensile strengths of concrete containing fly ash by GEP", *Comput. Concrete*, **17**(4), 489-498.
- Sarfarazi, V., Faridi, H. R., Haeri, H. and Schubert, W. (2016), "A new approach for measurement of anisotropic tensile strength of concrete", *Adv. Concrete Constr.*, **3**(4), 269-284
- Seeska, R., Lux, K.H. and Hesser, J.B.B. (2011), *Experiment: Long Term Deformation Behavior of Boreholes*, Mont Terri Technical Note TN 2011-04. Switzerland, Saint Ursanne.
- Shaowei, H., Aiqing, X., Xin, H. and Yangyang, Y. (2016), "Study on fracture characteristics of reinforced concrete wedge splitting tests", *Comput. Concrete*, **18**(3), 337-354.
- Shuraim, A.B., Aslam, F., Hussain, R. and Alhozaimy, A. (2016), "Analysis of punching shear in high strength RC panels-experiments, comparison with codes and FEM results", *Comput. Concrete*, **17**(6), 739-760.
- Sun, J.P., Zhao, Z.Y. and Zhang, Y. (2011), "Determination of three dimensional hydraulic conductivities using a combined analytical/neural network model", *Tunn. Undergr. Space Technol.*, **26**(2), 310-319.
- Tang, C.A. (1997), "Numerical simulation on progressive failure leading to collapse and associated seismicity", *Int. J. Rock Mech. Min. Sci.*, **34**(2), 249-262.
- Tang, C.A., Liu, H., Lee, P.K.K., Tsui, Y. and Tham, L.G. (2000), "Numerical studies of the influence of microstructure on rock failure in uniaxial compression part I: Effect of heterogeneity", *Int. J. Rock Mech. Min. Sci.*, **37**(4), 555-569.
- Tavallali, A. and Vervoort, A. (2010), "Effect of layer orientation on the failure of layered sandstone under Brazilian test conditions", *Int. J. Rock Mech. Min. Sci.*, **47**(2), 313-322.
- Tiang, Y., Shi, S., Jia, K. and Hu, S. (2015), "Mechanical and dynamic properties of high strength concrete modified with lightweight aggregates presaturated polymer emulsion", *Constr. Build. Mater.*, **93**, 1151-1156.
- Viotor, T., Li, X.L., Chen, G.J., Verstricht, J., Fisch, H. and Fierz, T. (2010), *Small Scale in Situ Tests: Bore-Hole Experiments at HADES and Mont Terri Concrete Laboratories*, Deliverable 8, TIMODAZ Project.
- Wang, Y.T., Zhou, X.P. and Shou, Y.D. (2017), "The modeling of crack propagation and coalescence in rocks under uniaxial compression using the novel conjugated bond-based peridynamics", *Int. J. Mech. Sci.*, **128**, 614-643.
- Wang, Y.T., Zhou, X.P. and Xu, X. (2016), "Numerical simulation of propagation and coalescence of flaws in rock materials under compressive loads using the extended non-ordinary state-based peridynamics", *Eng. Fract. Mech.*, **163**, 248-273.
- Wang, P.T., Yang, T.H., Xu, T., Cai, M.F. and Li, C.H. (2016), "Numerical analysis on scale effect of elasticity, strength and failure patterns of jointed rock masses", *Geosci. J.*, **20**(4), 539-549.
- Wasantha, P.L.P., Ranjith, P.G., Xu, T., Zhao, J. and Yan, Y.L. (2014), "A new parameter to describe the persistency of non-persistent joints", *Eng. Geol.*, **181**, 71-77.
- Yang, T.H., Wang, P.T., Xu, T., Yu, Q.L., Zhang, P.H., Shi, W.H. and Hu, G.J. (2015), "Anisotropic characteristics of fractured rock mass and a case study in Shirengou Metal Mine in China", *Tunn. Undergr. Space Technol.*, **48**, 129-139.
- Yang, T.H., Wang, P.T., Xu, T., Yu, Q.L., Zhang, P.H., Shi, W.H. and Hu, G.J. (2015), "Anisotropic characteristics of fractured rock mass and a case study in Shirengou Metal Mine in China", *Tunn. Undergr. Space Technol.*, **48**, 129-139.
- Yu, C., Deng, S.C., Li, H.B., Li, J.C. and Xia, X. (2013), "The anisotropic seepage analysis of water sealed underground oil storage caverns", *Tunn. Undergr. Space Technol.*, **38**, 26-37.
- Yun, T.S., Jeong, Y.J., Kim, K.Y. and Min, K.B. (2013), "Evaluation of rock anisotropy using 3D Xray computed tomography", *Eng. Geol.*, **163**, 11-19.
- Zhang, Q., Zhu, H.H., Zhang, L.Y. and Ding, X.B. (2011b), "Study of scale effect on intact rock strength using particle flow modeling", *Int. J. Rock Mech. Min. Sci.*, **48**(8), 1320-1328.
- Zhang, Z.X., Hu, X.Y. and Scott, K.D. (2011a), "A discrete numerical approach for modeling face stability in slurry shield tunnelling in soft soils", *Comput. Geotech.*, **38**(1), 94-104.
- Zhou, X.P., Xia, E.M., Yang, H.Q. and Qian, Q.H. (2012), "Different crack sizes analyzed for surrounding rock mass around underground caverns in Jinping I hydropower station", *Theoret. Appl. Fract. Mech.*, **57**(1), 19-30.
- Zhou, X.P., Zhang, Y.X. and Ha, Q.L. (2008), "Real-time computerized tomography (CT) experiments on limestone damage evolution during unloading", *Theoret. Appl. Fract. Mech.*, **50**(1), 49-56.
- Zhou, X.P., Shou, Y.D., Qian, Q.H. and Yu, M.H. (2014), "Three-dimensional nonlinear strength criterion for rock-like materials based on the micromechanical method", *Int. J. Rock Mech. Min. Sci.*, **72**, 54-60.
- Zhou, X.P. and Bi, J. (2018), "Numerical simulation of thermal cracking in rocks based on general particle dynamics", *J. Eng. Mech.*, **144**(1), 04017156.
- Zhou, X.P. (2010), "Dynamic damage constitutive relation of mesoscopic heterogenous brittle rock under rotation of principal stress axes", *Theoret. Appl. Fract. Mech.*, **54**(2), 110-116.

CC